Composites: Part B 53 (2013) 218–225

Contents lists available at SciVerse ScienceDirect

Composites: Part B

journal homepage: www.elsevier.com/locate/compositesb

Post buckling analysis of the shape memory polymer composite laminate bonded with alloy film

Tan Qiao [a], Liwu Liu [b], Yanju Liu [b], Jinsong Leng [a,*]

[a] Centre for Composite Materials, Science Park of Harbin Institute of Technology (HIT), P.O. Box 3011, No. 2 YiKuang Street, Harbin 150080, People's Republic of China
[b] Department of Astronautical Science and Mechanics, Harbin Institute of Technology (HIT), P.O. Box 301, No. 92 West Dazhi Street, Harbin 150001, People's Republic of China

ARTICLE INFO

Article history:
Received 17 January 2013
Received in revised form 26 March 2013
Accepted 7 April 2013
Available online 25 April 2013

Keywords:
B. Buckling
A. Laminates
C. Finite element analysis (FEA)
Numerical analysis

ABSTRACT

As a new kind of smart materials, shape memory polymer composites (SMPCs) are being used in large in-space deployable structures. However, the recovery force of pure SMPC laminate is very weak. In order to increase the recovery force of a SMPC laminate, an alloy film was bonded on the surface of the laminate. This paper describes the post bulking behavior of the alloy film reinforced SMPC laminate. The energy term associate with this in-plane post buckling have been given .Based on the theorems of minimum energy, a mathematical model is derived to describe the relation between the strain energy and the material and geometry parameters of the alloy film reinforced SMPC laminate. The finite element model (FEM) is also conducted to demonstrate the validity of the theoretical method. The relation between the recovery force and the material geometry parameters were also investigated. The presented analysis shows great potential in the engineering application such as deployment of space structures.

1. Introduction

Since the room inside a spacecraft is usually extremely limited, so reliable, lightweight and cost effective mechanisms for the enfoldment and deployment of trusses, solar arrays or other devices are needed [1–3]. Recently, a considerable interest has been placed on the use of shape memory polymer composites (SMPCs) [4,5], which are space-qualified, high deployed stiffness and high restoring strains and high strength-to-weight ratio making them appropriately used in constructing deployable space structures [6–8]. The shape memory polymer (SMP) and their composites can be bended and recovered when subjected to an external stimulus such as Joule heating, light, magnetism or moisture and so forth [9]. Among these SMP, the thermo-responsive SMP are the most common [10,11], which is usually heated through bonded on the surface of the SMPCs laminate with ohmic heating element.

Fiber post-buckling is a characteristic response that is occurred in the compression side of a SMPC laminate when the space structure has been packaged. Recently the buckling and post-buckling analyses for advanced composites, which are made by high modulus reinforcement with soft substrate, have been broadly studied [12–15]. In 2004, Chen et al. have elucidated nonlinear aspects of buckling behavior of composites at some periodic modes. Through the use of finite element method, it was found that the herringbone pattern has minimum energy among several patterns [16]. The wrinkles in a layered structure have been surveyed by Huang et al. The structure comprises of a stiff film bonded to a compliant substrate, which in turn is bonded to a rigid support. By minimizing energy, the wavelength and the amplitude of the wrinkles for different substrates with the consideration of their moduli and thicknesses have been obtained [17]. Post-micro-buckling behavior of elastic memory composite, expressions of the location of neutral strain surface, critical stress/strain and micro-buckle wavelength of SMPC laminate were studied by William in 2007 [18]. The buckling mechanics of silicon Nanowires (SiNWs) on elastomeric substrates were investigated by Ryu et al. [19]. In 2010, Xiao et al. developed a continuum mechanics theory for the in-surface buckling of one-dimensional nanomaterials on compliant substrates. Simple analytic expressions are obtained for the buckling wavelength, amplitude and critical buckling strain in terms of the bending and tension stiffness of nanomaterials [20].

It should be noted that the recovery force of pure SMPC laminate is not large enough to deploy the structure because of the friction among the deploying process of the space structures. Therefore, it is necessary to increase the recovery force of the laminate. Placing an alloy film on the surface of the laminate is an alternative way of increasing the recovery force. In addition, much of the previous works were focus on the post buckling response of the pure SMPC laminate, and relative little work has been done on the post buckling response of such a system. This research focus on the post-bulking behavior of the alloy film enforced SMPC laminate in a soft state.

* Corresponding author. Tel./fax: +86 451 86402328.
E-mail address: lengjs@hit.edu.cn (J. Leng).

1359-8368/$ - see front matter Crown Copyright © 2013 Published by Elsevier Ltd. All rights reserved.
http://dx.doi.org/10.1016/j.compositesb.2013.04.052

In this paper, the post buckling behavior of an alloy film reinforced SMPC laminate which can be used in actively deformable structures is investigated. A new style of post buckling theory that accounts for material parameters and geometrical character of the laminate and alloy film is established. The analytic solution is obtained via the minimum energy method for this post buckling response. The recovery force and recovery moment reinforcement function of the alloy film on the SMPC laminate have been discussed. This work discussed the reinforced effect of the recovery force and moment related to the alloy film on the SMPC laminate. In addition, the relation between the recovery force and geometry parameters (thickness and curvature) has also been investigated. The influence factors, such as the thickness of the alloy film, the curvature of the structure have also been investigated too.

2. Theoretical analysis

An alloy film was firstly bonded on the surface of the SMPC laminate, and then an external electric filed was applied on the alloy film. While at a temperature near or above the shape memory polymer's thermal transition temperature T_g, a certain bending strain was applied on the laminate. As illustrated in Fig. 1, the bending strain is realized through bending the laminate around cylinder. When the material is in rubber state, the stiffness of shape memory polymer matrix is reduced significantly and post buckling occurs at the compressed area of the laminate. The deformation mode performs shearing type buckling. Also as previously stated, fiber post-buckling is the primary deformation mode that allows soft-resin laminates to achieve high effective strains [21].

2.1. Structure strain energy

The cross section of the laminate is further divided into three areas. As illustrated in Fig. 2, in the range of $0 \leqslant z \leqslant z_{cb}$, when the laminate undergoes compression strain and fiber post buckling behavior occurs; in the area where $z_{cb} \leqslant z \leqslant z_{ns}$, the laminate only endure compression strain; in the range of $z_{ns} \leqslant z \leqslant z_h$, the laminate only subjects tensile strain. Plastic deformation and failure of the substrate and fiber have not been considered in the whole process.

Now derive energy expression of the fiber reinforced laminate with bonded electrical heating alloy film during the flexion deformity process. Supposing the fiber in the laminate as a beam, the bending of beams with moderately large rotations but with small strains can be derived using the principle of minimum energy principle. Assuming the fiber, alloy film and substrate of shape-memory material are linear elastic, the strain energy expression of body element ΔV can be approximated as follows:

$$\Delta U_s = 1/2\sigma_{ij}\varepsilon_{ij}\Delta V = 1/2(\sigma_{xx}\varepsilon_{xx} + \sigma_{yy}\varepsilon_{yy} + \sigma_{zz}\varepsilon_{zz} + \tau_{xy}\gamma_{xy} + \tau_{xz}\gamma_{xz} + \tau_{yz}\gamma_{yz})\Delta V \quad (1)$$

In the laminate's bending process, the strain ε_{xx} along the longitudinal direction is bigger than width strain ε_{yy} and radial strain ε_{zz}, thus the strain ε_{yy} and ε_{zz} can be ignored. Additionally, because *Y–Z* plane has been constrained rigidly by the cylinder, the shear strain γ_{yz} in *X–Z* plane can be ignored too. So strain energy of the substrate in Eq. (1) can be simplified as:

$$\Delta U_s = \Delta U_{xx} + \Delta U_{xy} + \Delta U_{xz} \quad (2)$$

In addition, to get the total energy of the whole system, the buckling strain energy of the fiber ΔU_f and tensile strain energy of alloy film ΔU_d need to be considered, thus the total energy expression can be described as following:

$$\Delta U_T = \Delta U_s + \Delta U_f + \Delta U_d = \Delta U_{xx} + \Delta U_{xy} + \Delta U_{yz} + \Delta U_f + \Delta U_d \quad (3)$$

2.2. Deformation process

Post buckling would likely occur at an inner face of a unidirectional fiber reinforced SMP laminate when it is subjected to bending moment [22,23]. To maintain the force equilibrium of the system, the neutral axis of the laminate will shift toward the outer surface of the laminate, thus realized the structure's large geometrical deflection deformation without failing [24]. Fiber post-buckling is a characteristic response that is occurred in the compression side of the laminate. It can be linear or non-linear depending on the strain level [25]. In the present study, *L*, *W* and *h* represent the length/widen and thickness of the laminate separately. Here, the SMPC laminate's permissible strain is $\varepsilon_{max} = 10\%$ thus the post buckling behavior is in linear elastic range.

According to the observation of William et al. [18], the initial shape of the fiber is straight. During the bending process, the initially straight reinforcement fibers deform into a wavy shape. And the wavy geometry appears to be sinusoidal in the plane of the laminate.

$$y = A\ \cos\left(\frac{\pi x}{\lambda}\right) \quad (4)$$

where *A* is the amplitude, and λ is the half-wave length. The fiber's macroscopic strain along *Y*-axis can be expressed as:

$$\varepsilon_{xx} = \frac{\Delta L}{L} = \frac{1}{2L}\int_0^L \left(\frac{\sqrt{(dx)^2 + (dy)^2} - dx}{dx}\right) dx \approx \frac{1}{2L}\int_0^L \left(\frac{dy}{dx}\right)^2 dx \quad (5)$$

As illustrated in Fig. 3, *L* denote the original length of the fiber, it is also the initial length of the laminate when it was fabricated. Initially, the reinforcement fibers are straight. During the bending process, the fiber which lay on the outside of the laminate micro-buckle, takes on a sine wavy geometry. And ΔL is the difference between fiber's initial length and the length after deformation.

According to Eqs. (1) and (2), it can be obtained:

$$\varepsilon_{xx} = \frac{1}{4}\left(\frac{A\pi}{\lambda}\right)^2 \quad (6)$$

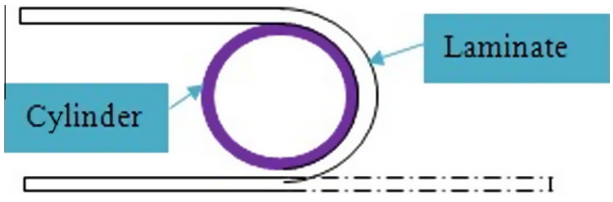

Fig. 1. Illustration of bending deformation for laminate.

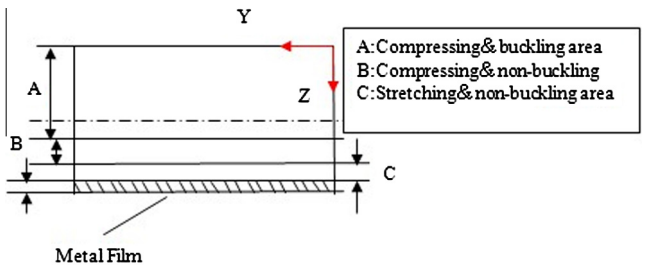

Fig. 2. Strain state of cross-section.

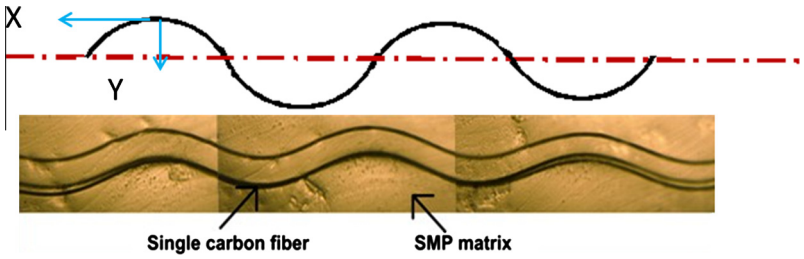

Fig. 3. The post-buckling of fiber reinforced SMP composite under compressive loading.

According to Eq. (6), we can derive the amplitude of the buckling wave as following:

$$A = 2\frac{\lambda}{\pi}\sqrt{-\varepsilon_{xx}} \tag{7}$$

Considering the laminate's deformation along negative Y axis, and according to composites plane theory, the strain ε_{xx} of the laminate can be obtained as:

$$\varepsilon_{xx} = k(z - z_{ns}) \tag{8}$$

where k is the curvature, Z_{ns} is the position of the neutral surface. Substitute Eq. (7) into Eq. (4), gives

$$y = 2\frac{\lambda}{\pi}\sqrt{k(z_{ns} - z)}\cos\left(\frac{\pi x}{\lambda}\right) \tag{9}$$

2.3. Flexural strain energy of fiber

Assuming the fiber in the laminate as a buckling beam and considering small strain and large displacement effect, the buckling strain energy equation of unidirectional fiber with length of L can be expressed as:

$$U_{(f\text{single fiber})} = \frac{1}{2}E_f I_f \int_0^L \left(\frac{d^2y}{dx^2}\right)^2 dx \tag{10}$$

Based on the experiment of Douglas Campbell, carbon fibers are distributed in the laminate evenly. At the shape memory's glass transition temperature, deform the sample along the cylinder, fibers within a polymer matrix can micro-buckle, taking on a sine wavy geometry and the fibers in Y direction undergo the same buckling deformation [26]. According to the investigate of Xin [27], the total buckling strain energy of the fibers can be evaluated as following:

$$U_f = \frac{2WLk\pi v_f E_f I_f}{\lambda^2 d^2} z_{cb}(2z_{ns} - z_{cb}) \tag{11}$$

where the symbols E_f, I_f, v_f stand for the Young's modulus, the moment of inertia, and Poisson's ratio respectively.

2.4. Shearing strain energy U_{xy}

In the bending deformation process of the laminate, the deformation along the circumference direction of the laminate has been constrained by the rigid cylinder, so the shearing strain energy U_{xy} of the substrate can be expressed as:

$$U_{xy} = \frac{1}{2}\int_0^{z_{cb}}\int_0^W\int_0^L v_s G_s \gamma_{xy}^2 dxdydz = v_s G_s kWz_{cb}L\left(z_{ns} - \frac{1}{2}z_{cb}\right) \tag{12}$$

In the above equation, W, L represent the laminate's width and length respectively, and v_s, G_s denote the Young's modulus and Poisson's ratio of the substrate.

2.5. Shearing strain energy U_{yz}

During the bending deformation process, the radial deformation of the laminate has been completely restrained, thus the displacement in Z direction equals to zero. Then the expressions of the substrates' shearing strain energy U_{yz} can be described as follows:

$$U_{yz} = \frac{1}{2}\int_0^{z_{cb}}\int_0^W\int_0^L v_s G_s \gamma_{yz}^2 dxdydz = \frac{LWk v_s G_s \lambda^2}{4\pi^2}\ln\left(\frac{z_{ns}}{z_{ns} - z_{cb}}\right) \tag{13}$$

2.6. Shearing strain energy

U_{xx} In the area of $z_{ns} \leqslant z \leqslant z_m$, the substrate and fiber is under tensile or compression strain. According to the parallel connection model of composites, the total strain energy of substrate and fiber in the area of $z_{ns} \leqslant z \leqslant z_m$ can be calculated as following by using the equal strain assumption:

$$\begin{aligned} U_{xx} &= \frac{1}{2}\int_{z_{cb}}^{z_m}\int_0^W\int_0^L E_{xx}\varepsilon_{xx}^2 dxdydz \\ &= \frac{1}{6}E_{xx}k^2LW[(z_m - z_{ns})^3 + (z_{ns} - z_{cb})^3] \end{aligned} \tag{14}$$

In which $E_{xx} = v_s E_s + v_f E_f$.

2.7. Shearing strain energy of the alloy film

The alloy film which has been bonded to the outer surface of the laminate only enduring tensile strain, hence, similar to the expression U_{xx} in Eq. (14), the strain energy of alloy film can be evaluated as follows:

$$\begin{aligned} U_d &= \frac{1}{2}\int_{z_m}^{t+z_m}\int_0^W\int_0^L E_m\varepsilon_{xx}^2 dxdydz \\ &= \frac{1}{6}E_m k^2 LW[(z_m + t - z_{ns})^3 + (z_{ns} - z_m)^3] \end{aligned} \tag{15}$$

2.8. Total strain energy

Thus the total energy can be expressed as:

$$U_T = U_d + U_{xx} + U_{xy} + U_{yz} + U_f \tag{16}$$

Therefore the total energy of the whole system is obtained as following:

$$\begin{aligned} U_T = {} & \frac{1}{6}E_m k^2 LW[(z_m + t - z_{ns})^3 + (z_{ns} - z_m)^3] + \frac{1}{6}E_{xx}k^2LW[(z_m - z_{ns})^3 \\ & + (z_{ns} - z_{cb})^3] + v_s G_s kWz_{cb}L\left(z_{ns} - \frac{1}{2}z_{cb}\right) \\ & + \frac{lwk v_m G_m \lambda^2}{4\pi^2}\ln\left(\frac{z_{ns}}{z_{ns} - z_{cb}}\right) + \frac{2WLk\pi v_f E_f I_f}{\lambda^2 d^2}z_{cb}(2z_{ns} - z_{cb}) \end{aligned} \tag{17}$$

3. Expressions of key parameter

The model parameters used in numerical example are listed in Table 1:

The relation of the total strain energy as a function of the parameters (z_{ns}/t) has been shown in Figs. 4 and 5. It is can be seen that U_{xx} and U_d decrease with the increasing of U_{xy}, U_{yz} and U_f, the minimum energy equilibrium point can be got from the sum of the five terms by using the principle of minimum energy.

The relationship between energy and the position of neutral surface is illustrated in Fig. 6. Comparing the total energy expression's first three items and the last two items to see which one is much smaller, therefore the model can be further simplified by neglecting the smallest one. The result shows that the curves $U_{xx}+U_{xy}+U_d$ and $U_{yz}+U_f+U_{xx}+U_{xy}+U_d$ are almost the same with the change of the neutral surface, therefore the last two terms $U_{yz}+U_f$, it's the energy terms of the fiber and the substrates' shearing strain energy can be ignored for simplicity.

Thus the total energy of the whole system can be simplified as:

$$U_T = \frac{1}{6}E_m k^2 LW[(z_m + t - z_{ns})^3 + (z_{ns} - z_m)^3] + \frac{1}{6}E_{xx}k^2 LW[(z_m - z_{ns})^3 + (z_{ns} - z_{cb})^3] + \nu_s G_s k W z_{cb} L\left(z_{ns} - \frac{1}{2}z_{cb}\right) \quad (18)$$

The minimum energy principle has been adopted to solve parameters z_{ns} and z_{cb}.

$$\begin{cases} \frac{\partial U_T(z_{ns},z_{cb})}{\partial z_{cb}} = 0 \\ \frac{\partial U_T(z_{ns},z_{cb})}{\partial z_{ns}} = 0 \end{cases} \quad (19)$$

According to Eq. (19), the analytical expression of the critical buckling position and neutral axis position can be derived as follows:

$$z_{ns} = z_m + \frac{E_m kt + \nu_s G_s - g}{E_{xx}k} \quad (20)$$

$$z_{cb} = z_m + \frac{E_m kt - \nu_s G_s - g}{E_{xx}k} \quad (21)$$

Table 1
Basic parameters for the component.

Parameter category	Geometric parameter				Material parameter
Parameter name	Length (cm)	Width (cm)	Thickness (cm)	Diameter (μm)	Modulus (GPa)
SMPC laminate	30.5	15.2	0.2		1
Alloy film	30.5	15.2	0.01		10
Fiber	30.5			7	230

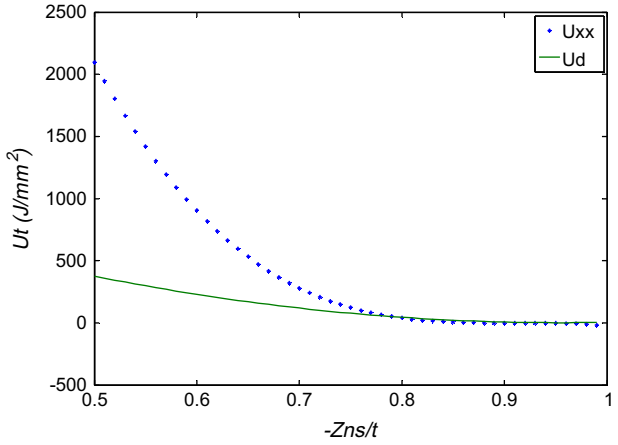

Fig. 4. Energy vs. ratio of neutral surface positions to thickness.

In which $g = \sqrt{(E_m kt)^2 + (G_s \nu_s)^2 + 2E_m kt G_s \nu_s + 2G_s \nu_s E_{xx} k z_m - E_{xx} k^2 E_m t^2}$

Variables z_{ns}, z_{cb} need to satisfy the condition of $0 \leqslant z_{cb} < z_{ns} < -t + z_m$, thus the following expression can be derived from Eq. (20) under the condition $0 \leqslant z_{cb}$:

$$k \leqslant \frac{4\nu_s G_s(E_{xx}z_m + E_m t)}{E_{xx}(E_m t^2 + 2E_m t z_m + E_{xx}z_m^2)} \quad (22)$$

Obviously, the fibers in substrate starting buckling only if $z_{cb} > 0$. Thus the critical curvature k_{cr} can be got when $z_{cb} = 0$:

$$k_{cr} = \frac{4\nu_s G_s(E_{xx}z_m + E_m t)}{E_{xx}(E_m t^2 + 2E_m t z_m + E_{xx}z_m^2)} \quad (23)$$

The critical curvature of the laminate without alloy film can be obtained by setting the thickness of the alloy film $t = 0$:

$$k_{cr} = \frac{4\nu_s G_s}{z_m E_{xx}} = \frac{4\nu_s G_s}{z_m(\nu_s E_s + \nu_f E_f)} \quad (24)$$

Because $\varepsilon_{xx} = k(z - z_{ns})$, the critical strain of the laminate can be expressed as:

$$\varepsilon_{cr} = k_{cr}(z - z_{ns}) = 4\frac{h}{fE_{xx}}\left[z - \left(1 + \frac{E_m t}{E_{xx}} - \frac{f}{h}(g + G_s \nu_s)\right)\right] \quad (25)$$

where f and h are:

$$h = \nu_s G_s(E_m t + E_{xx} z_m) \quad (26)$$

$$f = E_{xx}z_m^2 + E_m t^2 + 2E_m t z_m \quad (27)$$

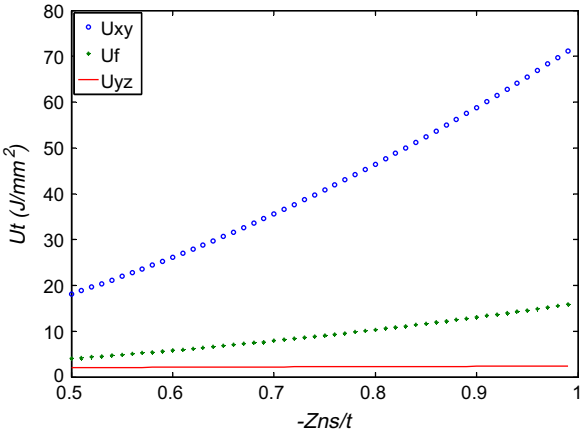

Fig. 5. Energy vs. ratio of neutral surface positions to thickness.

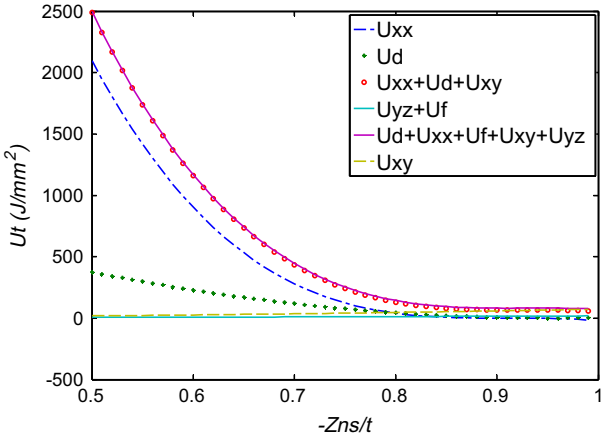

Fig. 6. Energy vs. ratio of neutral surface positions to thickness.

At the area of composite's compression micro buckling ($0 \leqslant z < z_{cb}$), the fiber's bulking amplitude A can be expressed as:

$$A = 2\frac{\lambda}{\pi}\sqrt{-\varepsilon_{xx}} \tag{28}$$

Substituting Eq. (25) into (28) gives:

$$A = 4\frac{\lambda}{\pi}\sqrt{\frac{h}{fE_{xx}}\left[\left(1+\frac{E_m t}{E_{xx}}-\frac{f}{h}(g+G_s\upsilon_s)\right)-z\right]} \tag{29}$$

The initial deformation is ignored and the deformation along Y negative direction is the only one to be considered, thus $\varepsilon_{yy} = 0$ and $\varepsilon_{zz} = 0$.

On the basis of composite plate theory, recovery moment can be evaluated as:

$$M_x = B_{ij}\varepsilon^0_{xx} + D_{ij}k \tag{30}$$

And the expression of recovery force can be expressed as:

$$N_x = A_{ij}\varepsilon^0_{xx} + B_{ij}k \tag{31}$$

where $\varepsilon^0_{xx} = kz_{ns}$, μ_{xx} denotes Poisson's ratio. B_{ij} is coupling stiffness, D_{ij} is bending stiffness.

Assuming the maximum strain absolute value of the laminate's inner side is $\varepsilon_{\max}$. The following relationship can be derived from Eq. (5):

$$4\frac{h}{fE_{xx}}\left(1+\frac{E_m t}{E_{xx}}-\frac{f}{h}(g+G_s\upsilon_s)\right) \leqslant \varepsilon_{\max} \tag{32}$$

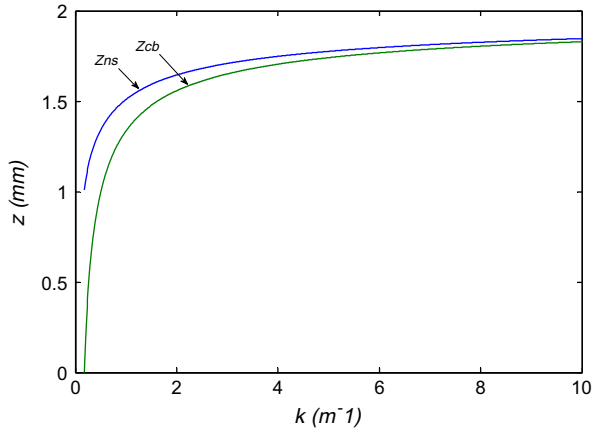

Fig. 7. Neutral plane and critical buckling position during the bending process.

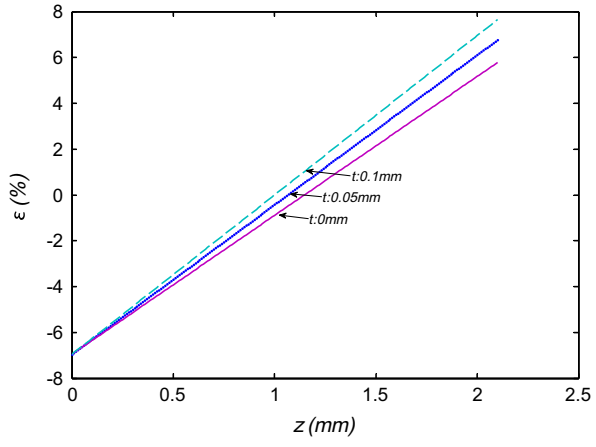

Fig. 8. Strain trends vs. position.

4. Results and discussion

As shown in Fig. 7, with the curvature increasing gradually, the location of critical buckling and the location of neutral surface changed correspondingly. Meanwhile, fiber buckling occurs at the inner compressive side of the laminate. As the curvature further increasing, z_{cb} and z_{ns} move toward the outer surface which subject to tensile stress. Meanwhile, z_{cb} moves toward to z_{ns} rapidly, which results in the decreasing of the compressing non-buckling area from initial value to zero gradually. Besides, to further investigate the effect of alloy film thickness on critical curvature, Fig. 10 has been plotted according to Eq. (24). It can be observed that when

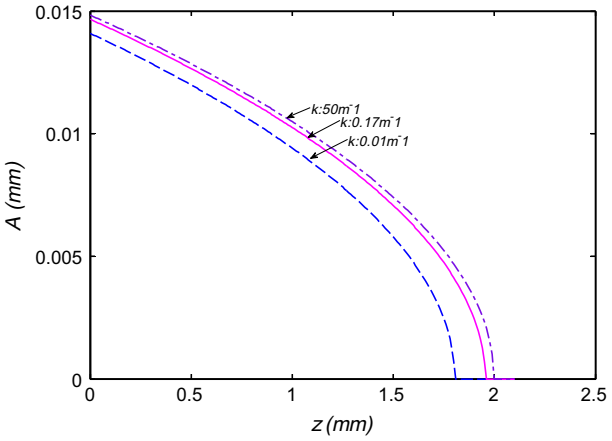

Fig. 9. Amplitude trends vs. curvature.

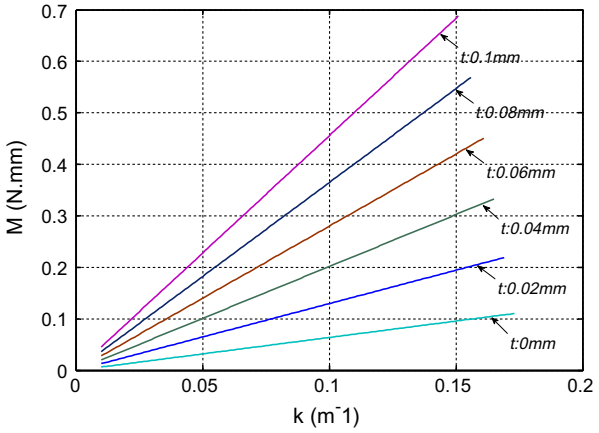

Fig. 10. Recovery moment vs. curvature.

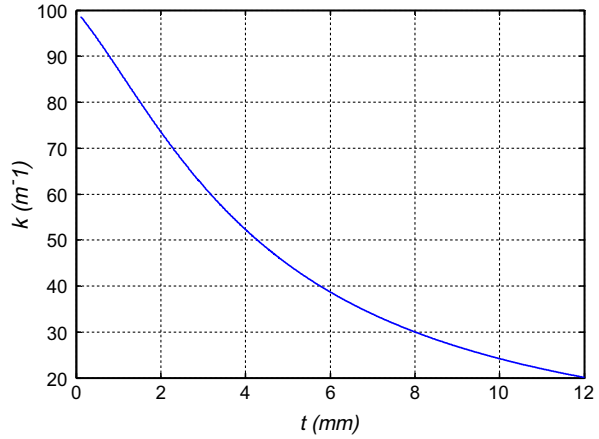

Fig. 11. Curvature vs. alloy film thickness.

the thickness of substrate is kept a constant, as the increasing of alloy film's thickness, the critical curvature decreases correspondingly.

The change trend of strain value along the thickness direction of the substrate is illustrated in Fig. 8. In the compressive side of the laminate, at the position of $z = 0$, the thickness value of alloy

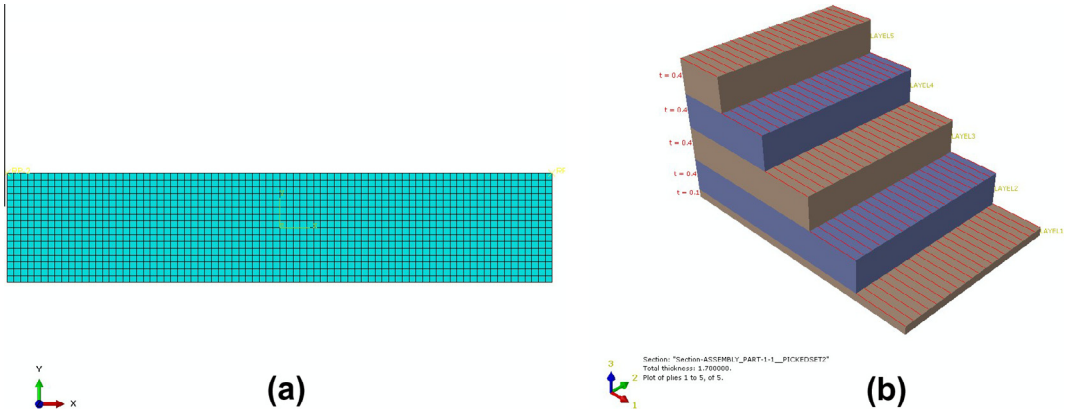

Fig. 12. Finite element model of the laminate (A) finite element meshes; (B) ply scheme.

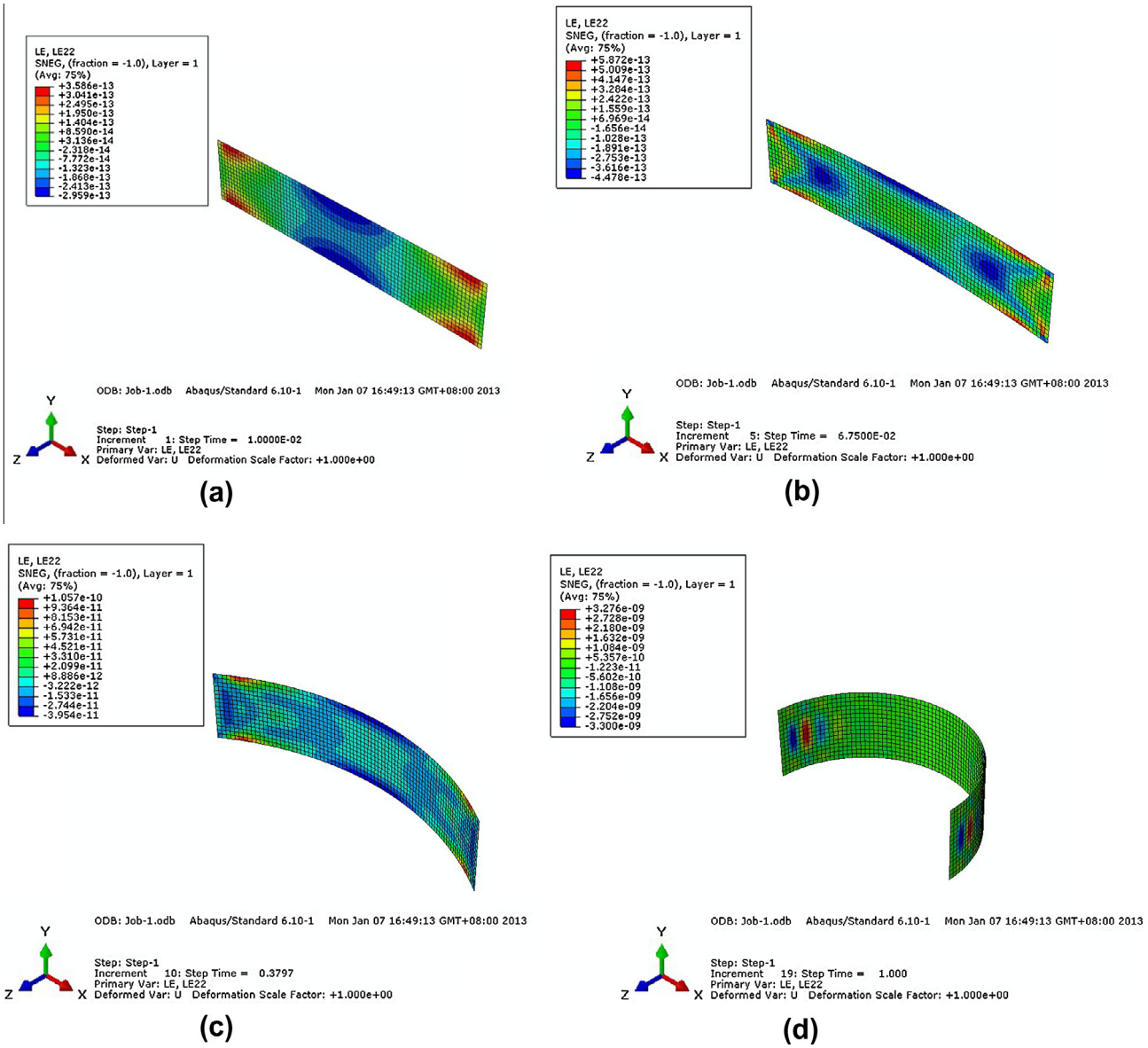

Fig. 13. Series strain distribution of the laminate from the bending sequence.

film is different while the strain value is the same. From the position of $z = 0$ to the laminate's neutral section, the value of compression strain continues to decline. Yet from neutral section to the outer tensile side of the laminate, tensile strain increase from zero gradually. Different alloy film thickness relates to different strain rate, as the alloy film thickness gets bigger, the strain rate gets smaller.

According to the Eq. (29), Fig. 9 reveals the distribution of fiber buckling amplitude in thickness direction with different curvature. At some fixed curvature, from the laminate's compressive side to neutral surface the amplitude decreases. At the position of $z = z_{ns}$, - the value of amplitude is zero. As the further increasing of the curvature, the neutral axis shifts to the outside of the laminate and at the same time, the amplitude increases as well.

Based on Eq. (30), the recovery moment is plotted in Fig. 10 as a function of curvature with different alloy film thicknesses. It is apparent that the recovery moment is highly dependent on alloy film thickness (Fig. 10). As the thickness of the alloy film increased from 0 mm to 0.1 mm, the recovery moment increased by approximate 10 times. Thus, bonded the SMPC laminate with alloy film can dramatically increase the recovery moment.

Because SMPCs laminate's permissible strain is $\varepsilon_{max} = 10\%$, based on Eq. (31), the allowable range of critical curvature k and alloy film thickness can be figured out. As illustrated in Fig. 11, with the increase of the laminate's permissible curvature, the thickness of alloy film needs to be deduced. More specifically, the permissible curvature and alloy film thickness must within the area under the curve. Otherwise, it will result in material failure.

5. Finite element model verify

Detailed simulations of the post buckling response of the SMPCs laminate have been carried out with the ABAQUS package. Thin shell elements have been used to model the laminate, and a 4-node reduced integration shell elements (S4R5) with 5° of freedom per node have been adopted, as it performs well for large rotations with only small strains.

Fig. 12 is the finite element model of the laminate. Fig. 13 shows a series of strains along X direction from the bending sequence of a uni-direction laminate with the same material properties and geometry of the theoretical model. The laminate is subjected to opposite-bending. As the thickness of the alloy film increases from 0.02 mm to 0.1 mm, the theory data and simulation result of the strain along X direction are given in Fig. 14, which illustrates that the simulation data agrees with theoretical value.

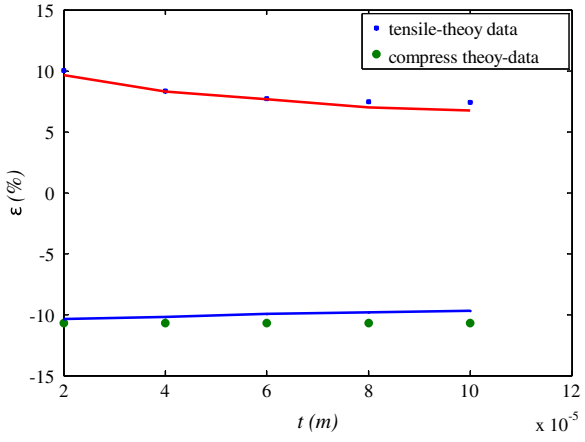

Fig. 14. Strain results for theory and simulation.

6. Conclusions

A theoretical model for the symmetric deformation of an alloy film reinforced SMPC laminate under a fixed curvature has been derived using a minimum energy principle. Using the proposed theory, a series of closed form solution of the location of neutral surface, critical curvature, recovery moment, and amplitude of the wavelength as a function of the prescribed curvature, geometry and material properties of the folded laminate was obtained. The recovery force and recovery moment reinforcement function of the alloy film geometry parameters (thickness and curvature) on the SMPC laminate have been investigated. It is reveals that as the thickness of the bonded alloy film increased from 0 mm to 0.1 mm, the recovery moment increased by almost 10 times. The allowable range of critical curvature and alloy film thickness have been figured out based on SMPCs laminate's permissible strain $\varepsilon_{max} = 10\%$. It is apparent that with the increase of the laminate's permissible curvature, the thickness of alloy film needs to be reduced. These conclusions and detailed analyses are essential for many future applications which use the reinforce behavior of alloy film in smart matrix composite laminate, such as deployable antenna, trusses, solar array. Next work will consider the non-linear response of the fiber and the thermal mechanical characteristic of the matrix.

Acknowledgements

This work is supported by the National Natural Science Foundation of China (Grant No. 11225211, No. 11272106, No. 11102052). We would also like to thank Dr. Kin-tak Lau for his great suggestions.

References

[1] Sokolowski WM, Tan SC. Advanced self-deployable structures for space applications. J Spacecr Rock 2007;44:750–4.
[2] Todoroki A, Kumagai K, Matsuzaki R. Self-deployable space structure using partially flexible CFRP with SMA wires. J Intell Mater Syst Struct 2009;20:1415–24.
[3] Lan X, Liu YJ, Lv HB, Wang XH, Leng JS, Du SY. Fiber reinforced shape-memory polymer composite and its application in a deployable hinge. Smart Mater Struct 2007;18:024002.
[4] Hollaway LC. Thermoplastic-carbon fiber composites could aid solar-based power generation: possible support system for solar power satellites. J Compos Constr 2011;15:239–47.
[5] Leng JS, Xin Lan, Liu YJ, Du SY. Shape-memory polymers and their composites: stimulus methods and applications. Prog Mater Sci 2011;56:1077–135.
[6] Dietsch B, Tong T. A review-features and benefits of shape memory polymers (SMPs). J Adv Mater 2007;39:3–12.
[7] Kim BK. Shape memory polymers and their future development. Exp Polym Lett 2008;2:614.
[8] Lendlein A, Schmidt AM, Schroeter M, Langer R. Shape-memory polymer networks from oligo(-caprolactone)dimethacrylates. J Polym Sci Part A – Polym Chem 2005;43:1369–81.
[9] Liu YJ, Lv HB, Lan X, Leng JS, Du SY. Review of electro-active shape-memory polymer composite. Compos Sci Technol 2009;69:2064–8.
[10] Li GQ, Xu W. Thermomechanical behavior of thermoset shape memory polymer programmed by cold-compression: testing and constitutive modeling. J Mech Phys Solids 2011;59:1231–50.
[11] Li GQ, Naveen U. Shape memory polymer based self-healing syntactic foam: 3-D confined thermomechanical characterization. Compos Sci Technol 2010;70:1419–27.
[12] Cai S, Breid D, Crosby AJ, Suo Z, Hutchinson JW. Periodic patterns and energy states of buckled films on compliant substrates. J Mech Phys Solids 2011;59:1094–114.
[13] Jiang HQ, Sun YG, Rogers JA, Huang YG. Post-buckling analysis for the precisely controlled buckling of thin film encapsulated by elastomeric substrates. Int J Solids Struct 2008;45:2014–23.
[14] Ryu SY, Xiao J, Park W, Son K, Huang Y, Paik U, et al. Lateral buckling mechanics in silicon nanowires on elastomeric substrates. Nano Lett 2009;9:3214–9.
[15] Xiao J, Ryu SY, Huang Y, Hwang KC, Paik U, Rogers JA. Mechanics of nanowire/nanotube in-surface buckling on elastomeric substrates. Nanotechnology 2010;21:085708.
[16] Chen X, Hutchinson JW. Herringbone buckling patterns of compressed thin films on compliant substrates. J Appl Mech 2004;71:597–603.

[17] Huang ZY, Hong W, Suo Z. Nonlinear analyses of wrinkles in a film bonded to a compliant substrate. J Mech Phys Solids 2005;53:2101–18.
[18] William HF, Mark SL, Marc RS, Douglas CM, Qi J. Elastic memory composite microbuckling mechanics: closed-form model with empirical correlation. In: Proceedings of AIAA-48 conference. Hawaii; April 2007. p.79–85.
[19] Ryu SY, Xiao JL, Park WI, Son KS, Huang YG, Paik U, et al. Lateral buckling mechanics in silicon nanowires on elastomeric substrates. Nano Lett 2009;9(9):3214–9.
[20] Xiao J, Ryu SY, Huang Y, Hwang KC, Paik U, Rogers JA. Mechanics of nanowire/nanotube in-surface buckling on elastomeric substrates. Nanotechnology 2010;21(8):1–9.
[21] Gall K, Mikulas M, Munshi NA, Beavers F, Tupper M. Carbon fiber reinforced shape memory polymer composites. J Intell Mater Syst Struct 2000;11:877–86.
[22] Kundu CK, Sinha PK. Post buckling analysis of laminated composite shells. Compos Struct 2007;78:316–24.
[23] Kundu CK, Maiti DK, Sinha PK. Post buckling analysis of smart laminated doubly curved shells. Compos Struct 2007;81:314–22.
[24] Song J, Jiang H, Liu ZJ, Khang DY, Huang Y, Rogers JA, et al. Buckling of a stiff thin film on a compliant substrate in large deformation. Int J Solids Struct 2008;45:3107–21.
[25] Anyfantis KN, Tsouvalis NG. Post buckling progressive failure analysis of composite laminated stiffened panels. Appl Compos Mater 2012;19:219–36.
[26] Douglas C, Arup M. Deployment precision and mechanics of elastic memory composites. In: Proceedings of AIAA-44 conference. Hawaii, April; 2003. p.1495.
[27] Lan X. Shape memory polymer composite and its study of mechanical foundations 2011:54–86.